Taylor & Francis
Taylor & Francis Group

Ships and Offshore Structures

ISSN: (Print) (Online) Journal homepage: https://www.tandfonline.com/loi/tsos20

Use of physical testing data for the accurate prediction of the ultimate compressive strength of steel stiffened panels

Hyun Ho Lee, Hyeong Jin Kim & Jeom Kee Paik

To cite this article: Hyun Ho Lee, Hyeong Jin Kim & Jeom Kee Paik (2023) Use of physical testing data for the accurate prediction of the ultimate compressive strength of steel stiffened panels, Ships and Offshore Structures, 18:4, 609-623, DOI: 10.1080/17445302.2022.2087358

To link to this article: https://doi.org/10.1080/17445302.2022.2087358

Published online: 22 Jun 2022.

SHIPS AND OFFSHORE STRUCTURES
2023, VOL. 18, NO. 4, 609–623
https://doi.org/10.1080/17445302.2022.2087358

Use of physical testing data for the accurate prediction of the ultimate compressive strength of steel stiffened panels

Hyun Ho Lee[a], Hyeong Jin Kim[a,b] and Jeom Kee Paik [b,c,d]

[a]Department of Naval Architecture and Ocean Engineering, Pusan National University, Busan, Republic of Korea; [b]Department of Mechanical Engineering, University College London, London, UK; [c]The Korea Ship and Offshore Research Institute (Lloyd's Register Foundation Research Centre of Excellence), Pusan National University, Busan, Republic of Korea; [d]School of Maritime and Transportation, Ningbo University, Ningbo, People's Republic of China

ABSTRACT

Physical testing data can be used to predict the ultimate compressive strength of steel stiffened panels. Moreover, useful empirical formulae have been developed by fitting curves to data from relevant testing databases. A representative example is the Paik–Thayamballi formula, which is based on physical testing data available until 1997 and is a closed-form function of plate and column slenderness ratios. Since 1997, high-precision data-acquisition equipment and large-scale physical models have been used to generate databases contained advanced testing data of modern materials such as AH32 high-tensile steel made by the thermo-mechanical control process (TMCP) technology together with modern fabrication technologies, e.g., flux-cored arc welding technique, under a strict control of welding parameters, e.g., current, voltage, speed and heat input, to achieve a required weld leg length. It is therefore important to determine if these advanced testing data are compatible with the established empirical formulae. This paper describes benchmark studies which were conducted to determine such compatibility, with a focus on the Paik–Thayamballi formula, and summarises key findings and insights obtained from the present study.

ARTICLE HISTORY
Received 11 November 2021
Accepted 3 June 2022

KEYWORDS
Ultimate compressive strength; steel stiffened plate structures; physical testing data; empirical formula; Paik–Thayamballi formula

1. Introduction

Steel stiffened panels are used as primary strength members in naval, offshore, mechanical, aerospace and civil engineering structures, and the ultimate limit states of such panels are currently used as the main criterion in safety assessments and structural design (Hughes and Paik 2010, Paik 2018, 2020, 2022). Various methods can be used to predict the ultimate strength of steel stiffened panels, such as analytical, semi-analytical, numerical, experimental and empirical methods. This ultimate strength is affected by a range of parameters, such as material and geometric properties; initial imperfections (e.g. initial deflection and welding-induced residual stress); in-service damage (e.g. corrosion wastage, fatigue cracking and local denting); accident-induced damage (e.g. collision or grounding damage); the presence of cut-outs; sub-zero or elevated temperatures; and loading speed (Paik 2020, 2022).

This paper does not present a review of research on steel stiffened panels or aluminium-stiffened panels; these can be found in the literature such as Zhang (2014) and Hosseinnabadi and Khedmati (2021), respectively. In addition, a large number of recent studies have examined the ultimate strength of steel stiffened panels (e.g. Abdussamie et al. 2018, Anyfantis 2020, Ao et al. 2020, Bhudia 2019, Cui and Wang 2020, Eslami-Majd and Rahbar-Ranji 2015, Fanpourgakis and Samuelides 2021, Feng et al. 2020, 2021, Georgiadis and Samuelides 2021, Han et al. 2021, He et al. 2020, Jagite et al. 2019, 2021, Kim et al. 2009, 2018a, 2018b, 2019, Lee and Paik 2020, Li et al. 2021a, 2021b, Liu et al. 2021a, 2021b, Ma and Wang 2021, Paik et al. 2020a, 2020b, 2021a, 2021b, 2021c, Piculin and Može 2021, Putranto et al. 2021, Rahbar-Ranji and Zarookian 2015, Ringsberg et al. 2021, Ryu et al. 2021, Shi and Gao 2021a, 2021b, Shi et al. 2021, Sohn et al. 2016, Xu and Soares 2021, Xu et al. 2019, 2021, Yi et al. 2019, 2020, 2021, and Zhang et al. 2020).

Rather, this study focuses on the applicability of the Paik-Thayamballi empirical formula developed by a curve-fitting of physical test data, which can be used for predicting the ultimate compressive strength of steel stiffened panels. It did so by exploiting certain physical test data that have been obtained for steel panels (aluminium alloy panels are beyond the scope of this study) at room temperature (20°C). These data are listed in the below-mentioned databases described in Section 3, and are for panels containing the following features:

- identically spaced longitudinal stiffeners;
- typical types of stiffeners (i.e. flat, angle or Tee-bar);
- welding-induced initial imperfections (e.g. initial plate deflections, initial distortions of stiffeners and residual stresses);
- no in-service damage or accident-induced damage;
- no openings or cut-outs; and
- static axial compressive loadings without dynamic effects in the direction of longitudinal stiffeners.

2. Geometric and material properties influencing ultimate compressive strength

Structural characteristics must be identified to enable the ultimate compressive strength of stiffened panels to be predicted. Hull structures in ships and offshore installations are mainly formed from stiffened plate structures and support members, such as longitudinal stiffeners and transverse frames, all of which are described by the nomenclature listed in Figure 1 (Hughes and Paik 2010, Paik 2018).

CONTACT Jeom Kee Paik j.paik@ucl.ac.uk Department of Mechanical Engineering, University College London, London, UK

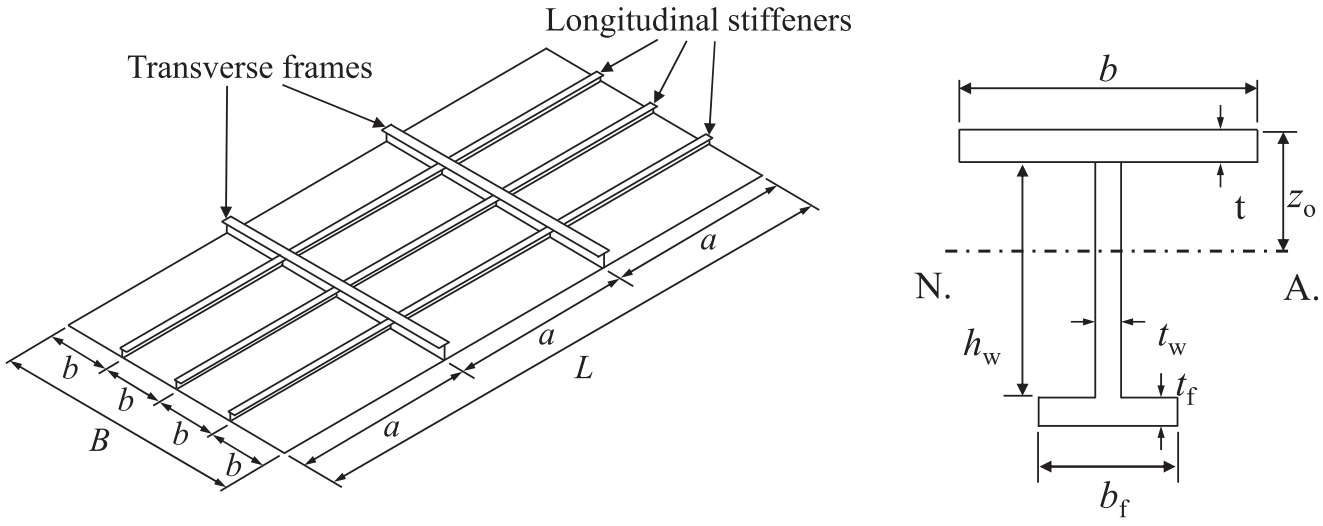

Figure 1. Schematic and nomenclature of dimensions of a stiffened panel and a support member.

Steel stiffened panels can be characterised by the plate slenderness ratio β and the column slenderness ratio of longitudinal stiffeners with attached plating, λ (Paik 2018). These two parameters are defined as follows:

$$\beta = \frac{b}{t}\sqrt{\frac{\sigma_{Yp}}{E}} \tag{1a}$$

$$\lambda = \frac{a}{\pi r}\sqrt{\frac{\sigma_{Yeq}}{E}} \tag{1b}$$

where a is the plate length (the spacing between transverse frames); b is the plate breadth (the spacing between longitudinal stiffeners); t is the plate thickness; E is Young's modulus; σ_{Yp} is the yield strength of the plate material; and r is the radius of gyration of the longitudinal stiffener with attached plating, which is calculated as $r = \sqrt{I/A}$ (where I is the moment of inertia and A is the cross-sectional area).

The yield strength of a plate usually differs from that of its stiffeners. Thus, σ_{Yeq} in Equation (1b) is the equivalent yield strength over the cross-section of the stiffeners with attached plating, and is defined as

$$\sigma_{Yeq} = \frac{A_p\sigma_{Yp} + A_w\sigma_{Yw} + A_f\sigma_{Yf}}{A} \tag{2}$$

where σ_{Yp} is the yield stress of plating; σ_{Yw} is the yield stress of web; and σ_{Yf} is the yield stress of flange. Also, $A = A_p + A_w + A_f$, $A_p = bt$, $A_w = h_w t_w$ and $A_f = b_f t_f$ in which b is the plate breadth (stiffener spacing), t is the thickness of plating, h_w is the stiffener web height, t_w is the stiffener web thickness, .b_f is the stiffener flange breadth and t_f is the stiffener web thickness.

Equations (3a) and (3b) define the moment of inertia (I) for a stiffener attached to plating and the distance from the outer surface of attached plating to its neutral axis (z_o), respectively:

$$I = \frac{bt^3}{12} + bt\left(z_o - \frac{t}{2}\right)^2 + \frac{h_w^3 t_w}{12} + h_w t_w\left(z_o - t - \frac{h_w}{2}\right)^2 + \frac{b_f t_f^3}{12} + b_f t_f\left(t + h_w + \frac{t_f}{2} - z_o\right)^2 \tag{3a}$$

$$z_o = \frac{0.5bt^2 + h_w t_w(t + 0.5h_w) + b_f t_f(t + h_w + 0.5t_f)}{bt + h_w t_w + b_f t_f} \tag{3b}$$

However, there are two types of moment of inertia for a stiffener attached to plating: using stiffener spacing and effective width as the breadth of attached plating. The former is already mentioned in Equation (3), and the latter can be calculated by substituting stiffener spacing with the effective width. The effective width is an important concept because it can characterise the ineffectiveness of attached plating as a result of non-uniform stress distribution (Paik 2018).

There is a need to investigate the properties of stiffened panels in as-built trading ships, and Figures 2 and 3 present the geometric properties of stiffened panels in various sizes of as-built containerships and oil tankers, respectively. It can be seen that the ranges of the plate and column slenderness ratios in these ships are 0.5–5.0 and 0.25–1.0, respectively.

A stiffened panel under predominantly compressive loads may exhibit a variety of failure modes before it reaches its ultimate strength. Paik and Thayamballi (2003) originally defined failure in terms of the following six categories of collapse modes (Paik 2018):

- Mode I: Overall collapse of plating and stiffeners as a unit
- Mode II: Plate collapse without distinct failure of stiffeners
- Mode III: Beam–column collapse
- Mode IV: Collapse by local web buckling of stiffeners
- Mode V: Collapse by lateral-torsional buckling of stiffeners (tripping)
- Mode VI: Gross yielding

Mode I collapse occurs if a panel's stiffeners are relatively weak. In Mode II, a panel collapses by yielding along the plate–stiffener intersection at its edges, with no stiffener failure occurring. In Mode III, the ultimate strength is reached due to yielding of the plate–stiffener combination at its mid-span. Modes IV and V involve stiffener-induced failure that occurs when the ratio of the stiffener web height to the stiffener web thickness is large and/or when the type of stiffener flange cannot remain straight, such that the stiffener web buckles or twists sideways. Mode VI occurs when a panel has extremely low slenderness is (i.e. the panel is extremely stocky) and/or when the panel is subjected predominantly to axial tensile loading.

Figure 4 presents the collapse modes of stiffened panels in as-built containerships and oil tankers. These modes were obtained

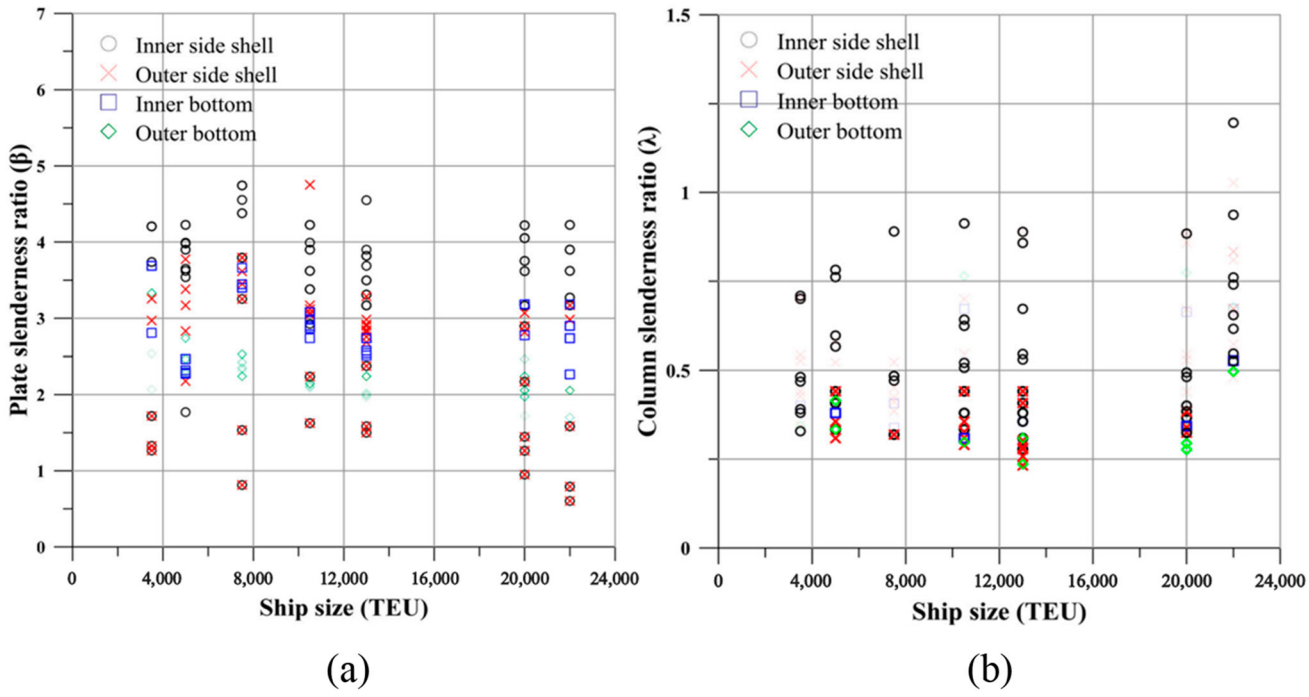

Figure 2. Geometric properties of stiffened panels in various sizes of as-built containerships: (a) plate slenderness ratio, and (b) column slenderness ratio.

using the Analysis of Large Plated Structures/Ultimate Limit State Assessment Program (ALPS/ULSAP 2021), and are based on the assumption that the panels were predominantly subjected to axial compressive loads. In this figure, all the ultimate compressive strength normalised by yield strength is in a range of 0.6–0.9, and it can be seen that all the panels are collapsed in mode III or V as shown in Figure 4. The collapse of modes III and V typically occurs when the dimensions of stiffeners are intermediate, neither weak nor very strong and when a stiffener flange is unable to remain straight so that a stiffener web twists sideways, respectively (Hughes and Paik 2010, Paik 2018).

3. Collection of physical testing data

Advancements in manufacturing technologies (e.g., flux-cored arc welding technique under a strict control of welding parameters such as current, voltage, speed and heat input to achieve a required weld leg length) have led to modern materials (e.g., TMCP steels)

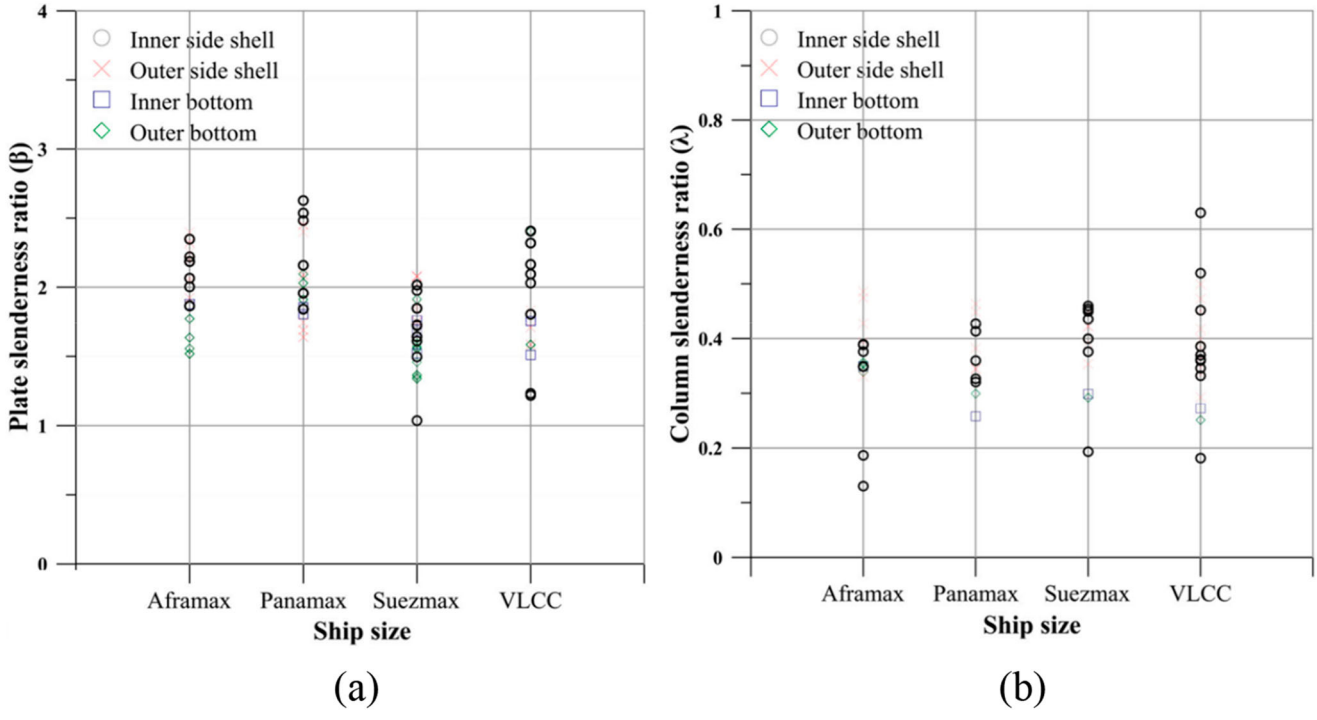

Figure 3. Geometric properties of stiffened panels in various sizes of as-built oil tankers: (a) plate slenderness ratio, and (b) column slenderness ratio.

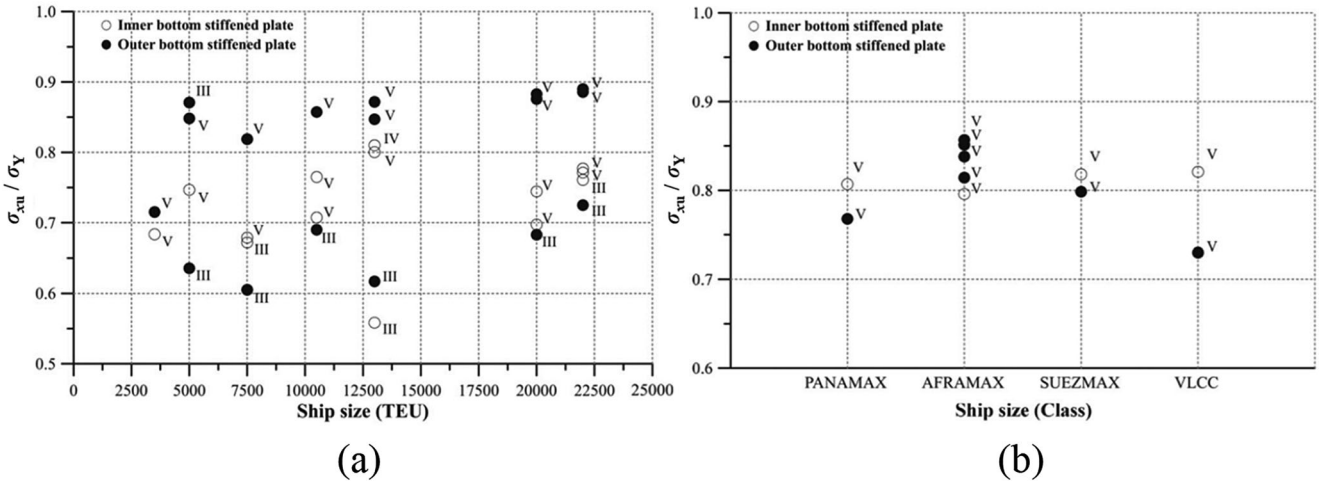

Figure 4. Collapse modes of steel stiffened panels (obtained using the Analysis of Large Plated Structures/Ultimate Limit State Assessment Program) in as-built: (a) containerships, and (b) oil tankers.

with enhanced properties and also welding technologies have been advanced to maximise the weld performance and minimise the fabrication-related initial imperfections (Paik 2022). To consider this aspect, physical data from recent testing studies (published after 1997) with modern materials were used in the Paik–Thayamballi empirical formula to determine its suitability for application to modern materials (as the Paik–Thayamballi empirical formula was devised using physical testing data acquired up to 1997). The studies that obtained these recent physical testing data are summarised in the following paragraphs and Table 1.

Paik et al. (2020b) conducted full-scale collapse testing of the bottom structures of a 1,900 TEU containership. They found that the effect of cyclic axial compressive loading on the ultimate limit states of steel stiffened panels is negligible if the cyclic loading does not lead to low-cycle fatigue cracking and/or the collapse of local structural members. However, this may not be true for cyclic loading that leads to structural behaviours different from those described above (Jagite et al. 2019, 2021; Paik 2022; Jagite and Bigot 2022). Figure 5 shows photographs of a structure that exhibited Mode V collapse (due to the tripping of stiffeners) when subjected to full-scale collapse testing.

Ringsberg et al. (2021) presented a benchmark study on the ultimate limit state analysis of steel stiffened plate structures. The benchmark study was initiated and coordinated by the ISSC 2022 Technical Committee III.1-Ultimate Strength, and focused on the predictions of the buckling collapse and ultimate compressive strength of stiffened panels. The benchmark study by a participation of 17 teams was performed in 3 phases distinguished by the level of information, and results of numerical simulations for individual 3 phases were compared with reference experimental data to investigate the influence of uncertainties in the computational modelling procedure, material properties, and initial imperfections on the predictions of the ultimate strength. The overall length of the reference experimental structure was 7315 mm and the width was 2438 mm, and the plating consisted of two full-breadth parts: 6.35 mm thick plating with a length of 3352 and 7.94 mm thick plating with a length of 3962 mm joined in the middle section by a butt weld. Stiffeners of the reference structure were composed of three longitudinal stiffeners, a single longitudinal girder and four transverse frames as shown in Figure 6(a). Figure 6 shows a schematic diagram of the reference test structure and a deformed shape of the test structure after the ultimate strength was reached, showing tripping of the girder and local flange buckling of the longitudinal stiffeners.

Table 1. Physical testing studies published since 1997 on the ultimate compressive strength of stiffened panels.

No.	Authors	Publication year	Size	Number of specimens	Type of stiffener(s)
1	Paik et al.	2020	Full scale	1	Tee
2	Choi et al.	2009	Small scale	9	Flat, Tee
3	Chujutalli et al.	2020	Small scale	10	Flat, Tee
4	Gordo and Guedes Soares	2008	Small scale	8	Angle, Flat
5	Manco et al.	2019	Small scale	6	Angle
6	Ringsberg et al.	2021	Full scale	1	Tee
7	Woloszyk et al.	2020	Small scale	3	Tee
8	Xu and Soares	2021	Small scale	6	Angle

Choi et al. (2009) conducted physical tests to examine the collapse behaviour of nine stiffened panels, and validated the effectiveness of the Structural Stability Research Council-type critical stress curve through a comparative analysis with the physical testing results. Chujutalli et al. (2020) performed collapse tests to examine the ultimate compressive strength and behaviour of damaged stiffened panels, and performed numerical simulations to investigate the influence of indentation parameters. Gordo and Soares (2008) conducted physical tests to examine the ultimate compressive strength and behaviour of stiffened panels with various combinations of mechanical material properties, stiffener types and panel widths. Furthermore, Manco et al. (2019), Woloszyk et al. (2020) and Xu and Soares (2021) experimentally investigated the influences of corrosion, plate/column slenderness ratio and number of stiffeners, respectively, on the collapse behaviour of stiffened panels. Figures 7 and 8 show the deformed stiffened panels after collapse tests in the abovementioned studies.

Physical testing data are generally useful for predicting and validating the ultimate strength of stiffened panels and for providing insights into structural responses for use in safety assessments. Thus, physical testing data reported until 1997 are provided in Tables 2–6 as additional information.

4. Paik–Thayamballi empirical formula

Paik and Thayamballi (1997) examined the physical testing data published until 1997 (as indicated in Tables 2–7) to build a database to establish an empirical formula for predicting the ultimate strength of steel stiffened panels. To consider the practical and

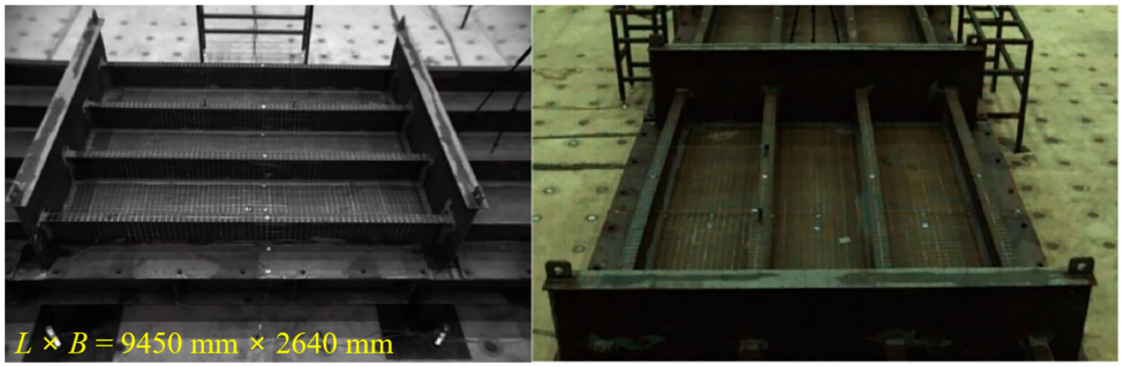

(a)

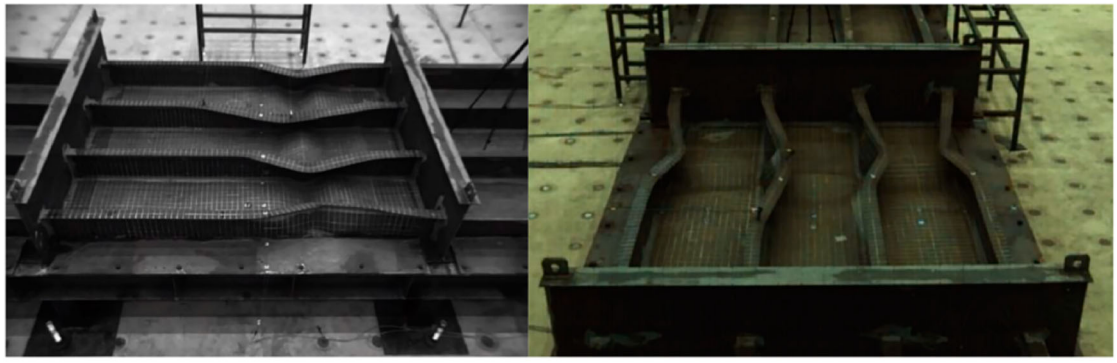

(b)

Figure 5. Structure (a) before and (b) after full-scale collapse testing (Paik et al. 2020b).

conservative characteristics of the derived empirical formula, data from physical tests in which simply supported conditions were set as boundary conditions were investigated. Furthermore, Paik and Thayamballi conducted 10 physical tests with small dimension stiffeners to ensure that the empirical formula has a wide range of applications for a plate slenderness of 0.701-4.088 and a column slenderness ratio of 0.251-2.021. The resulting empirical formula for predicting the ultimate strength of steel stiffened panels is given in Equation (4). This improved version of the formula proposed by Lin (1985) is based on the built database and uses the least-squares method, and implicitly accounts for the influence of welding-induced initial imperfections. Because the inputs λ and β are determined for the complete plating section, it is not necessary to evaluate the effective width of the attached plating.

$$\frac{\sigma_{xu}}{\sigma_{Yeq}} = \frac{1}{\sqrt{0.995 + 0.936\lambda^2 + 0.170\beta^2 + 0.188\lambda^2\beta^2 - 0.067\lambda^4}} \quad (4)$$

where σ_{xu} is the ultimate strength of the stiffened panels, σ_{Yeq} is the equivalent yield strength over the cross-section, and λ and β denote the column and plate slenderness ratios, respectively, of the plate–stiffener combination section. Because the ultimate strength of the column must be less than the elastic column buckling strength (by Euler buckling strength formula), $\sigma_{xu}/\sigma_{Yeq} = 1/\lambda^2$ if $\sigma_{xu}/\sigma_{Yeq} > 1/\lambda^2$.

5. Validation of the Paik–Thayamballi empirical formula

The Paik–Thayamballi empirical formula was derived from physical testing data published up until 1997. Therefore, in this study, the Paik–Thayamballi empirical formula was applied to physical testing data obtained since 1997 (as specified in Section 3) to validate the formula's applicability. In addition, a comparative analysis was performed by applying empirical formulae derived from numerical simulations to the recent physical testing data, to provide supplementary information. The empirical formulae based on numerical simulations are described in the following paragraphs.

Kim et al. (2017) used results of numerical simulations and statistical techniques to develop an empirical formula (Equation (5)) based on column and plate slenderness ratios and two correction coefficients. One hundred and twenty-four steel stiffened panels were considered in the simulation scenarios, and 2-bay–2-span models were used to perform the numerical simulations, to alleviate the effect of the boundary conditions.

$$\frac{\sigma_{xu}}{\sigma_{Yeq}} = \frac{1}{0.8884 + e^{\lambda^2}} + \frac{1}{0.4121 + e^{\sqrt{\beta}}} \quad (5)$$

Xu et al. (2018) developed an empirical formula that considers the influence of the lateral pressure (Equation (6)). This formula is based on the results of 1296 numerical simulations, and is composed of the column and plate slenderness ratios and 11 correction coefficients (where the latter depend on the water head (in meters) and the stiffener type).

$$\frac{\sigma_{xu}}{\sigma_{Yeq}} = \frac{1}{\sqrt{c_0 + c_1\lambda + c_2\beta + c_3\lambda\beta + c_4\lambda^2 + c_5\beta^2 + c_6\lambda^2\beta^2 + c_7\lambda^3 + c_8\beta^3 + c_9\lambda^3\beta^3 + c_{10}\lambda^4}} \quad (6)$$

Zhang and Khan (2009) developed an empirical formula for predicting the ultimate compressive strength of steel stiffened panels

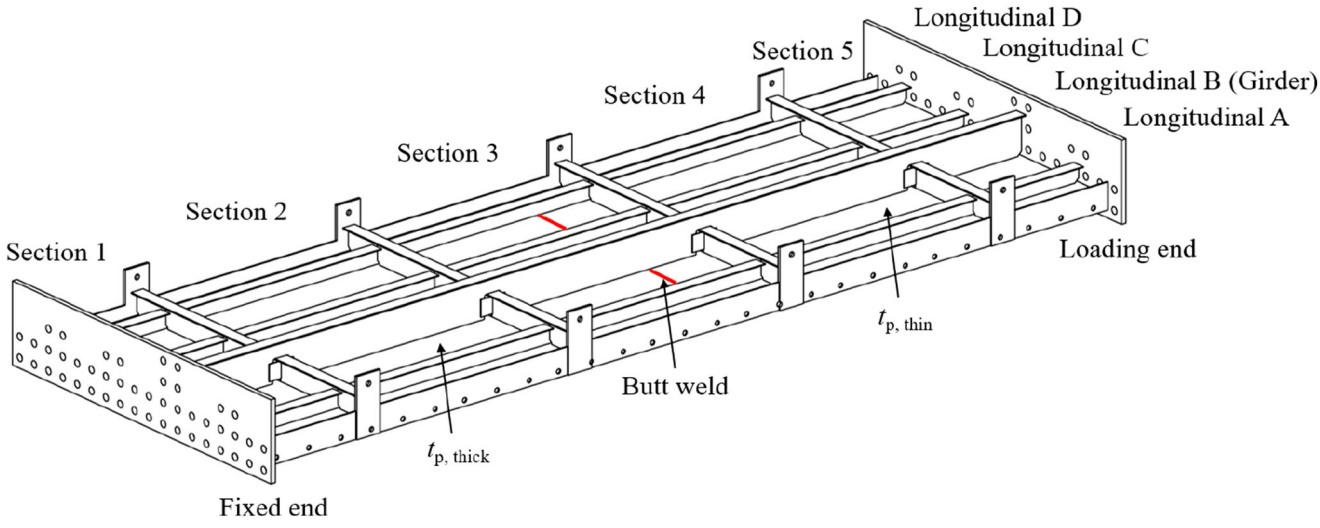

(a)

(b)

Figure 6. (a) A schematic diagram of the reference structure and (b) a deformed shape after the test structure reached the ultimate strength (Ringsberg et al. 2021).

(Equation (7)). This formula was derived from observations of the collapse patterns of steel stiffened panels and by considering numerical simulation results.

$$\frac{\sigma_{xu}}{\sigma_{Yeq}} = \frac{1}{\beta^{0.28}} \cdot \frac{1}{\sqrt{1+\lambda^{3.2}}} \tag{7}$$

The stiffened plate structure used for the benchmark study of Ringsberg et al. (2021) had a non-uniform plate thickness and different longitudinal stiffener scantlings, and thus it was idealised with an uniform plate thickness and identical longitudinal stiffener scantlings under a condition of the equal cross-sectional area. This may cause some modelling uncertainties.

Figure 9 presents comparisons of the ultimate compressive strengths of stiffened steel panels measured in recent physical testing and predicted using the aforementioned empirical formulae. In the figure, the 80% and 60% (dashed lines and dash-dotted lines, respectively) represent the range of differences between the measured and predicted values. In most cases, there was a difference of less than 20% between the ultimate compressive strengths predicted using the Paik–Thayamballi formula and those measured in recent physical testing. Except in a

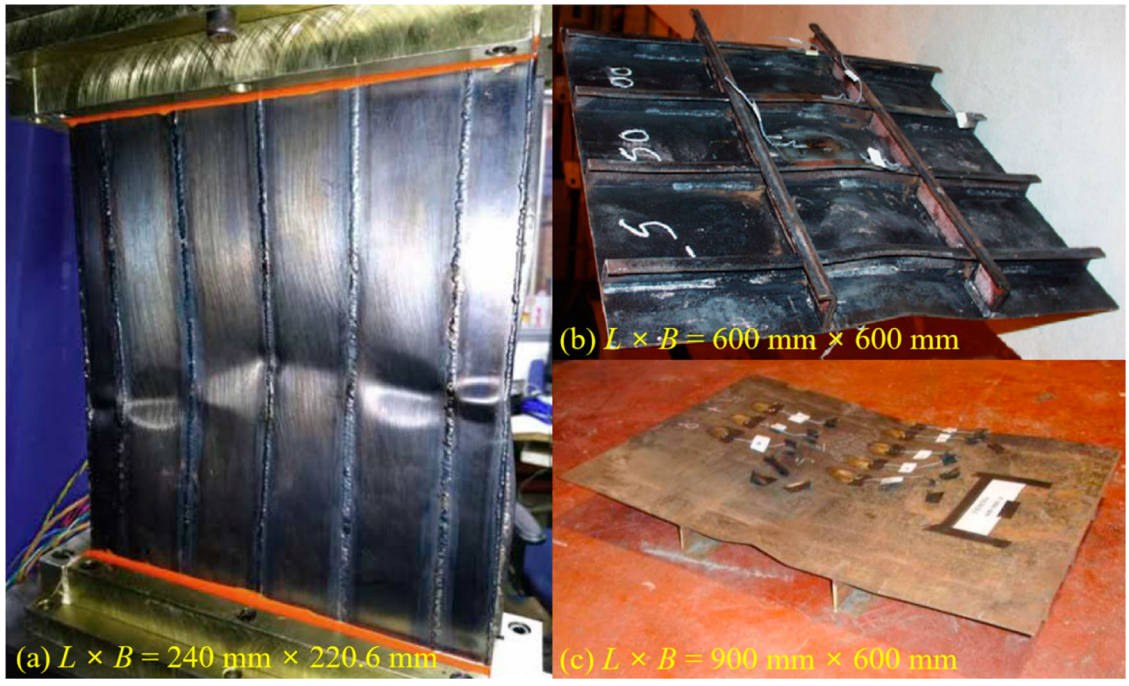

Figure 7. Deformed stiffened panels after collapse tests (1/2) (a) Chujutalli et al. (2020), (b) Gordo and Guedes Soares (2008), (c) Xu and Guedes Soares (2021).

few cases, a similar difference was found between ultimate compressive strengths predicted by empirical formulae based on numerical simulations and those measured in recent physical testing.

All of the empirical formulae were quantitatively evaluated in terms of the mean and coefficient of variation (COV) of the data gradients, as shown in Figure 9. A mean close to one and a COV close to zero indicated a high agreement between the ultimate compressive strengths predicted by empirical formulae and measured in recent physical testing. The Zhang–Khan formula exhibited the lowest mean error (2.3%), followed by the Xu empirical formula (5.9%). Moreover, the recent physical testing data and the empirical formulae-generated values exhibit excellent agreement: all formulae had COVs within 0.2. The empirical formula proposed by Xu et al. had the lowest COV (0.115), followed by the Zhang–Khan empirical formula (0.127). As shown in Figure 9, the full-scale testing data were the testing data that are most consistent with the results generated by the empirical formulae. This confirms that all of the empirical formulae could accurately predict the ultimate compressive strength of stiffened panels, even in full-scale structures.

Figure 8. Deformed stiffened panels after collapse testing (2/2) (a) Manco et al. (2019), (b) Woloszyk et al. (2020).

Figure 10 presents a comparison of the ultimate compressive strengths of stiffened panels predicted by the empirical formulae and measured in all physical tests (i.e. both recent (since 1997) and previous (up until 1997) physical testing data (see section 3)). The recent and previous physical testing data are similarly dispersed, but compared to recent testing data, there are more sets of previous testing data that are greater than 20% different from the data generated by empirical formulae. These greater differences were statistically clarified by calculating means and COVs with and without the inclusion of previous data (Table 8). The mean errors and COVs increased for most of the empirical formulae when the previous data were included i.e. the agreement between the measured and predicted values worsened. The testing-based empirical formulae, i.e. the Paik–Thayamballi empirical formula, exhibited the highest agreement with all of the physical testing data, as indicated by its having the lowest mean error of 3.3% and COV of 0.147. Moreover, most of the other empirical formulae predicted the ultimate compressive strengths with reasonable accuracy (COVs = 0.2 and mean errors $\leq$ 10%). However, the empirical formula proposed by Xu et al. tended to overestimate ultimate compressive strengths by approximately 24% (relative to all of the physical testing data).

6. Concluding remarks

This study examined the applicability of the Paik–Thayamballi empirical formula, which is based on physical testing data reported up until 1997, to data for materials obtained by current advanced

Table 2. Physical testing data published up until 1997 on the ultimate compressive strengths of steel stiffened panels (Horne et al. 1976, 1977).

Specimen No.	a (mm)	B (mm)	n_{st}	b (mm)	t (mm)	h_w (mm)	t_w (mm)	b_f (mm)	t_f (mm)	w_{op}/t_p	w_{os}/a ($\times 10^{-3}$)	λ	β	σ_{rc}/σ_{Yp}	σ_{Yp}	σ_{Ys}	σ_{Yeq}	σ_{xu}/σ_{Yeq}	Failure Mode	
3(FB)	915	1,371	2	457	9.5	152.5	9.5	–	–	0.13	1.85	0.251	1.708	0.129	259.5	275.1	263.4	0.854	IW	III
7(FB)	1,830	1,371	2	457	9.5	152.5	16.0	–	–	0.18	0.30	0.440	1.692	0.412	254.7	268.1	259.5	0.794	CW	II
8(FB)	1,830	1,371	2	457	9.5	152.5	16.0	–	–	0.09	0.38	0.442	1.717	0.125	262.1	262.0	262.1	0.851	IW	II
9(FB)	1,830	1,371	2	457	9.5	152.5	9.5	–	–	0.08	0.30	0.504	1.717	0.122	262.1	272.5	264.7	0.782	IW	III
11(FB)	1,830	1,371	2	457	9.5	152.5	16.0	–	–	0.19	0.66	0.449	1.760	0.120*	275.5	262.0	270.6	0.791	IW	II
12(FB)	1,830	1,371	2	457	9.5	152.5	16.0	–	–	0.27	0.52	0.440	1.692	0.418*	254.7	268.1	259.5	0.794	CW	II
13(FB)	1,830	1,371	2	457	9.5	152.5	16.0	–	–	0.61	0.27	0.449	1.760	0.120*	275.5	262.0	270.6	0.750	IW	II
14(FB)	1,830	1,371	2	457	9.5	152.5	16.0	–	–	0.63	0.46	0.440	1.692	0.418*	254.7	268.1	259.5	0.832	CW	II
A11(FB)	1,830	1,371	2	457	6.5	152.5	9.5	–	–	0.89	0.44	0.538	0.971	0.120*	367.4	334.7	356.7	0.544	IW	II
A12(FB)	1,830	1,371	2	457	6.5	152.5	9.5	–	–	0.23	0.66	0.534	2.897	0.066	349.3	354.5	351.0	0.569	IW	II
A21(FB)	1,830	1,371	2	457	6.5	152.5	9.5	–	–	0.88	1.39	0.527	2.879	0.418*	345.2	334.7	341.8	0.642	CW	II
A22(FB)	1,830	1,371	2	457	6.5	152.5	9.5	–	–	0.22	0.66	0.518	2.832	0.418*	334.0	323.9	330.7	0.564	CW	II
A23(FB)	1,830	1,371	2	457	6.5	152.5	9.5	–	–	0.23	0.90	0.528	2.909	0.424	352.2	323.9	342.9	0.608	CW	II
D11(FB)	1,830	1,371	2	457	10.0	80.0	12.0	–	–	0.54	0.68	1.096	1.694	0.120*	282.9	290.7	284.3	0.632	IW	II
D12(FB)	1,830	1,371	2	457	10.0	80.0	12.0	–	–	0.31	0.60	1.001	1.540	0.132	233.6	252.3	236.8	0.648	IW	II
D21(FB)	1,830	1,371	2	457	10.0	80.0	12.0	–	–	0.57	0.38	1.018	1.570	0.418*	243.0	256.0	245.3	0.574	CW	II
D22(FB)	1,830	1,371	2	457	10.0	80.0	12.0	–	–	0.12	0.44	1.032	1.575	0.315	244.3	287.0	251.7	0.600	CW	II
E11(FB)	1,830	1,371	2	457	6.5	76.0	12.5	–	–	0.97	0.44	1.148	2.840	0.120*	335.9	374.0	345.1	0.471	IW	II
E12(FB)	1,830	1,371	2	457	6.5	76.0	12.5	–	–	0.26	0.49	1.148	2.835	0.088	334.7	377.9	345.2	0.476	IW	II
E21(FB)	1,830	1,371	2	457	6.5	76.0	12.5	–	–	0.86	0.98	1.139	2.839	0.418*	335.6	353.3	339.9	0.443	CW	II
E23(FB)	1,830	1,371	2	457	6.5	76.0	12.5	–	–	0.38	0.93	1.139	2.815	0.33	329.8	369.5	339.4	0.448	CW	II
AF2(A)	3,000	600	2	200	10.3	152.0	6.5	76.0	9.8	0.08	0.20	0.606	0.805	0,418*	353.5	410.2	379.4	0.892	CW	III
AF3(A)	3,000	600	2	200	10.1	152.0	6.5	76.0	10.1	0.11	0.40	0.593	0.779	0.594	318.4	426.2	368.5	0.739	CW	III
AS2(A)	3,000	600	2	200	10.4	152.0	6.6	38.0	12.0	0.10	0.43	0.659	0.816	0.418*	366.6	409.7	384.4	0.812	CW	III
AS3(A)	3,000	600	2	200	10.4	152.0	6.5	76.0	11.75	0.09	0.40	0.601	0.821	0.458	375.2	422.4	397.6	0.660	CW	III
BF2(B)	3,000	600	2	200	10.0	160.0	8.0	–	–	0.11	0.47	0.737	0.790	0.418*	320.8	302.8	313.8	0.613	CW	III
BF3(B)	3,000	600	2	200	10.1	160.0	8.0	–	–	0.08	0.30	0.759	0.796	0.545	332.4	329.3	331.2	0.546	CW	III
FS4(FB)	3,000	600	2	200	9.9	148.5	9.8	–	–	0.05	0.27	0.850	0.838	0.120*	353.7	410.3	377.7	0.681	IW	III
FS5(FB)	3,000	600	2	200	10.1	148.5	9.8	–	–	0.10	0.40	0.867	0.842	0.191	372.0	417.7	391.1	0.595	IW	III
FS9(FB)	3,000	600	2	200	9.9	148.5	9.8	–	–	0.09	0.57	0.840	0.828	0.418*	345.7	400.6	369.0	0.754	CW	III
FSI0(FB)	3,000	600	2	200	9.9	148.5	9.8	–	–	0.09	0.80	0.844	0.832	0.568	348.8	403.7	372.1	0.709	CW	III
PF2(FB)	2,700	600	2	200	9.7	150.0	15.2	–	–	0.07	0.41	0.728	0.858	0.556	356.1	408.3	384.3	0.787	CW	II
PF5(FB)	2,700	900	2	300	10.0	150.0	15.2	–	–	0.14	0.26	0.790	1.344	0.329	413.3	415.6	414.3	0.791	CW	II
PF11(FB)	2,700	1,050	2	350	9.8	150.0	15.2	–	–	0.16	0.39	0.784	1.532	0.219	378.8	410.1	391.3	0.750	CW	II
SWI(FB)	2,700	1,440	2	480	9.7	150.0	15.2	–	–	0.19	0.41	0.839	2.132	0.102	382.1	428.3	397.3	0.717	IW	II
SW3(FB)	2,700	1,440	2	480	9.7	150.0	15.2	_	–	0.28	0.44	0.838	2.138	0.177	384.2	421.8	396.5	0.714	IW	II
SW5(FB)	2,700	1,440	2	480	9.7	150.0	15.2	.	–	0.20	0.30	0.851	2.204	0.269	408.4	408.8	408.5	0.636	CW	II
SW7(FB)	2,700	1,440	2	480	9.7	150.0	15.2	–	–	0.14	0.30	0.866	2.229	0.067	417.7	434.1	423.1	0.693	IW	II

n_{st} = The number of longitudinal stiffeners; w_{op} = The maximum magnitude of plate initial deflection; and w_{os} = The maximum magnitude of stiffener sideways initial distortion.

Table 3. Physical testing data published up until 1997 on the ultimate compressive strengths of steel stiffened panels (Faulkner 1977).

Specimen No.	a (mm)	B (mm)	n_{st}	b (mm)	t (mm)	h_w (mm)	t_w (mm)	b_f (mm)	t_f (mm)	w_{op}/t_p	w_{os}/a ($\times 10^{-3}$)	λ	β	σ_{rc}/σ_{Yp}	σ_{Yp}	σ_{Ys}	σ_{Yeq}	σ_{xu} / σ_{Yeq}	Failure Mode
P1(T)	244	530.4	5	88	3.07	17.4	4.88	12.7	6.17	0.13	0.20	0.314	1.004	0.178	250.0	283.0	262.4	0.976	II
P2(T)	384	882	5	147	2.62	30.4	4.83	12.7	6.22	0.47	0.10	0.330	1.956	0.178	250.0	262.0	254.4	0.733	II
P3(T)	638	1326	5	221	2.54	54.1	4.90	12.7	6.10	1.11	0.33	0.346	3.069	0.178	256.0	247.0	252.6	0.713	IV
P4(T)	523	1416	5	236	2.01	43.6	4.80	12.7	6.25	1.86	0.31	0.324	3.848	0.178	221.0	250.0	232.0	0.567	II
P5(T)	488	530.4	5	88	3.07	17.4	4.88	12.7	6.17	0.03	2.46	0.597	0.952	0.178	225.0	259.0	237.8	0.824	II
P6(T)	767	882	5	147	2.62	30.4	4.83	12.7	6.22	0.29	1.01	0.648	1.912	0.178	239.0	259.0	246.4	0.750	II
P7(T)	1275	1326	5	221	2.54	54.1	4.90	12.7	6.10	0.58	0.85	0.703	3.152	0.178	270.0	246.0	260.9	0.621	IV
P8(T)	1046	1416	5	236	2.01	43.6	4.80	12.7	6.25	1.36	0.47	0.675	4.068	0.178	247.0	259.0	251.5	0.515	II
P9(T)	732	530.4	5	88	3.07	17.4	4.88	12.7	6.17	0.12	2.43	0.918	0.963	0.178	230.0	283.0	249.9	0.716	II
P10(T)	1151	882	5	147	2.62	30.4	4.83	12.7	6.22	0.45	1.33	0.972	1.912	0.178	239.0	258.0	246.0	0.660	II
P11(T)	1913	1326	5	221	2.54	54.1	4.90	12.7	6.10	1.08	1.76	1.020	2.965	0.178	239.0	252.0	243.9	0.494	II
P12(T)	1570	1416	5	236	2.01	43.6	4.80	12.7	6.25	2.05	0.72	1.020	4.084	0.178	249.0	266.0	255.4	0.448	II
PI3(FB)	262	530.4	5	88	3.10	26.4	3.10	–	–	0.12	0.15	0.405	1.000	0.178	253.0	261.0	254.8	0.988	II
P14(T)	244	1062	5	177	3.05	17.5	4.85	12.7	6.15	0.49	0.29	0.356	2.990	0.178	242.0	269.0	248.3	0.764	II
P15(T)	422	1590	5	265	3.07	33.9	4.95	12.7	6.20	1.03	0.36	0.376	2.867	0.178	227.0	267.0	236.3	0.569	II
P16(T)	384	1770	5	295	2.57	30.5	4.90	12.7	6.12	1.93	0.18	0.386	3.952	0.178	244.0	273.0	250.7	0.506	II
P17(T)	523	530.4	5	88	3.10	26.4	3.10	–	–	0.03	0.71	0.777	0.951	0.178	229.0	256.0	235.2	0.822	II
P18(T)	488	1062	5	177	3.05	17.5	4.85	12.7	6.15	0.2	0.39	0.690	1.936	0.178	229.0	246.0	232.9	0.656	II
P19(T)	843	1590	5	265	3.07	33.9	4.95	12.7	6.2	0.65	0.42	0.781	3.027	0.178	253.0	266.0	256.0	0.563	II
P20(T)	767	1770	5	295	2.57	30.5	4.90	12.7	6.12	0.83	0.31	0.782	4.088	0.178	261.0	247.0	257.8	0.455	II
P21(FB)	785	530.4	5	88	3.10	26.4	3.10	–	–	0.12	1.12	1.223	1.010	0.178	258.0	262.0	258.9	0.696	II
P22(T)	732	1062	5	177	3.05	17.5	4.85	12.7	6.15	0.48	0.55	1.065	0.990	0.178	242.0	262.0	246.6	0.515	II
P23(T)	1265	1590	5	265	3.07	33.9	4.95	12.7	6.20	1.08	0.64	1.154	2.972	0.178	244.0	262.0	248.2	0.491	II
P24(T)	1151	1770	5	295	2.57	30.5	4.90	12.7	6.12	1.89	0.45	1.145	3.912	0.178	239.0	267.0	245.5	0.384	II
FI(FB)	348	1374	5	229	2.54	38.1	9.53	–	–	1.08	–	0.307	2.961	0.178	222.0	238.0	228.1	0.566	II
F2(FB)	653	1374	5	229	2.54	38.1	9.53	–	–	1.14	5.28	0.591	2.994	0.178	227.0	262.0	240.5	0.577	II
F3(FB)	958	1374	5	229	2.54	38.1	9.53	–	–	1.02	3.58	0.822	2.775	0.178	195.0	250.0	216.1	0.459	II
F4(FB)	1,262	1374	5	229	2.54	38.1	9.53	–	–	0.93	–	1.030	2.725	0.178	188.0	208.0	195.7	0.339	II
FL(FB)	577	816	5	136	4.93	63.5	3.02	–	–	0.07	0.43	0.434	1.089	0.178	321.0	321.0	321.0	0.779	IV
FLIS(FB)	577	272	1	136	4.93	63.5	3.02	–	–	0.14	–	0.434	1.089	0.178	321.0	321.0	321.0	0.752	IV
FL2(FB)	577	816	5	136	4.93	63.5	3.02	–	–	0.11	0.35	0.376	0.956	0.178	247.0	219.0	240.8	0.787	IV
FL2S(FB)	577	272	1	136	4.93	63.5	3.02	–	–	0.11	–	0.376	0.956	0.178	247.0	219.0	240.8	0.723	IV
TI(T)	1224	1218	5	203	1.98	35.0	4.95	13.0	6.35	0.59	0.46	0.823	3.115	0.178	190.0	208.0	197.0	0.390	II
T2(T)	874	1014	5	169	1.98	25.4	4.95	13.3	6.35	0.27	0.09	0.797	2.580	0.178	188.0	278.0	222.7	0.352	II
T3(T)	986	1212	5	202	1.91	34.8	4.95	13.3	6.35	0.39	0.33	0.638	3.162	0.178	184.0	184.0	184.0	0.416	II
T4(T)	704	996	5	166	2.08	25.4	4.95	13.2	6.35	0.25	0.47	0.656	2.463	0.178	196.0	287.0	230.4	0.403	II
T5(T)	1019	954	5	159	2.41	35.6	5.08	13.3	6.35	0.01	0.95	0.656	2.062	0.178	201.0	267.0	228.0	0.619	II
T6(T)	1110	1278	5	213	2.54	50.8	4.45	12.7	6.23	1.01	–	0.626	2.905	0.178	247.0	247.0	247.0	0.610	II
TT(T)	775	942	5	157	2.41	35.6	4.95	13.3	6.25	0.02	0.79	0.573	2.257	0.178	247.0	262.0	253.1	0.558	II
T8(T)	546	696	5	116	3.09	25.4	4.95	13.23	6.25	0.21	–	0.532	1.308	0.178	250.0	267.0	256.3	0.744	II
T9(T)	673	1038	5	173	3.07	44.5	4.90	12.7	6.25	0.05	0.75	0.446	1.999	0.178	259.0	293.0	271.2	0.634	II
T10(T)	376	690	5	115	3.10	25.4	4.95	12.7	6.25	0.23	–	0.391	1.397	0.178	292.0	279.0	287.3	0.879	II
T11(T)	409	492	5	82	4.32	25.4	4.95	12.7	6.25	0.06	–	0.411	0.701	0.178	281.0	283.0	281.7	0.820	II

Table 4. Physical testing data published up until 1997 on the ultimate compressive strengths of steel stiffened panels (Niho 1978).

Specimen No.	a (mm)	B (mm)	n_{st}	b (mm)	t (mm)	h_w (mm)	t_w (mm)	b_f (mm)	t_f (mm)	w_{op}/t_p	w_{os}/a ($\times 10^{-3}$)	λ	β	σ_{rc}/σ_{Yp}	σ_{Yp}	σ_{Ys}	σ_{Yeq}	σ_{xu} / σ_{Yeq}	Failure Mode
F20A(FB)	600	600	3	150	3.27	20	3.27	–	–	0.31	6.59	1.711	1.779	0.475	309.7	309.7	309.7	0.550	III
F20R(FB)	600	600	3	150	3.27	20	3.27	–	–	0.31	9.86	1.737	1.807	0.460	319.5	319.5	319.5	0.386	III
F30A(1)(FB)	600	600	3	150	3.27	30	3.27	–	–	0.31	0.95	1.031	1.779	0.475	309.7	309.7	309.7	0.644	II
F30R(1)(FB)	600	600	3	150	3.27	30	3.27	–	–	0.31	1.65	1.047	1.807	0.460	319.5	319.5	319.5	0.645	II
F30R(2)(FB)	600	600	3	150	3.27	30	3.27	–	–	0.31	2.74	1.047	1.807	0.460	319.5	319.5	319.5	0.595	II
F45R(FB)	600	600	3	150	3.27	45	3.27	–	–	0.31	1.09	0.629	1.807	0.460	319.5	319.5	319.5	0.633	II
T45R(T)	600	600	3	150	3.27	25	3.27	20	3.27	0.31	0.70	1.317	1.807	0.460	319.5	319.5	319.5	0.612	II

Table 5. Physical testing data published up until 1997 on the ultimate compressive strengths of steel stiffened panels (Yao 1980).

Specimen No.	a (mm)	B (mm)	n_{st}	B (mm)	t (mm)	h_w (mm)	t_w (mm)	b_f (mm)	t_f (mm)	w_{op}/t_p	w_{os}/a ($\times 10^{-3}$)	λ	β	σ_{rc}/σ_{Yp}	σ_{Yp}	σ_{Ys}	σ_{Yeq}	σ_{xu} / σ_{Yeq}	Failure Mode
STY-1(FB)	500	500	1	250	3.13	18.50	3.13	–	–	0.07	0.44	2.021	3.244	0.330	339.4	339.4	339.4	0.305	III
STY-2(FB)	500	500	1	250	3.13	20.45	3.13	–	–	0.09	0.56	1.785	3.244	0.330	339.4	339.4	339.4	0.337	III
STY-3(FB)	500	500	1	250	3.13	22.40	3.13	–	–	0.06	0.38	1.592	3.244	0.330	339.4	339.4	339.4	0.336	III
STY-4(FB)	500	500	1	250	3.13	23.50	3.13	–	–	0.05	0.31	1.498	3.244	0.330	339.4	339.4	339.4	0.370	III
STY-5(FB)	500	500	1	250	3.13	25.0	3.13	–	–	0.10	0.63	1.383	3.244	0.330	339.4	339.4	339.4	0.382	III
STY-6(FB)	500	500	1	250	3.13	27.80	3.13	–	–	0.02	0.13	1.206	3.244	0.330	339.4	339.4	339.4	0.446	II
STY-7(FB)	500	500	1	250	3.13	38.34	3.13	–	–	0.15	0.94	0.792	3.244	0.330	339.4	339.4	339.4	0.449	II

Table 6. Physical testing data published up until 1997 on the ultimate compressive strengths of steel stiffened panels (Tanaka and Endo 1988).

Specimen No.	a (mm)	B (mm)	n_{st}	b (mm)	t (mm)	h_w (mm)	t_w (mm)	b_f (mm)	t_f (mm)	w_{op}/t_p	w_{os}/a ($\times 10^{-3}$)	λ	β	σ_{rc}/σ_{Yp}	σ_{Yp}	σ_{Ys}	σ_{Yeq}	σ_{xu} / σ_{Yeq}	Failure Mode
D0(FB)	1080	1440	3	360	6.15	110	9.77	–	–	0.016	–	0.367	1.975	0.088	234.2	287.1	251.5	0.931	IV
D0A(FB)	1080	1440	3	360	5.65	110	10.15	–	–	0.044	–	0.343	2.220	0.088	249.9	196.0	230.8	0.843	IV
D1(FB)	1080	1200	3	300	5.95	110	10.19	–	–	0.024	–	0.350	1.771	0.102	253.8	250.9	252.7	1.095	IV
D2(FB)	1080	1560	3	390	5.95	110	10.19	–	–	0.048	–	0.369	2.302	0.073	253.8	250.9	252.9	0.900	IV
D3(FB)	1080	1440	3	360	5.95	103.5	11.84	–	–	0.524	–	0.397	2.125	0.091	253.8	326.3	280.2	1.032	IV
D4(FB)	1080	1440	3	360	5.95	118.5	7.98	–	–	0.020	–	0.357	2.125	0.134	253.8	284.2	263.1	0.990	IV
D4A(FB)	1080	1440	3	360	5.65	118.5	8.08	–	–	0.067	–	0.349	2.220	0.134	249.9	274.4	257.7	0.875	IV
D10(FB)	1080	1200	3	300	4.38	65	4.38	–	–	0.118	–	1.028	3.174	0.084	442.0	442.0	442.0	0.547	IV
D11(FB)	1080	1200	3	300	4.38	90	4.38	–	–	0.115	–	0.678	3.174	0.057	442.0	442.0	442.0	0.527	IV
D12(FB)	1080	1440	3	360	4.38	65	4.38	–	–	0.119	–	1.097	3.089	0.085	442.0	442.0	442.0	0.510	IV

Table 7. Physical testing data published until 1997 on the ultimate compressive strength of steel stiffened panels (Paik and Thayamballi 1997).

Specimen No.	a (mm)	B (mm)	n_{st}	b (mm)	t (mm)	h_w (mm)	t_w (mm)	b_f (mm)	t_f (mm)	w_{op}/t_p	w_{os}/a ($\times 10^{-3}$)	λ	β	σ_{rc}/σ_{Yp}	σ_{Yp}	σ_{Ys}	σ_{Yeq}	σ_{xu} / σ_{Yeq}	Failure Mode
SP3-1(FB)	500	500	1	250	3.5	17.5	3.5	–	–	0.47	3.12	1.987	2.729	0.330	300.5	300.5	300.5	0.399	III
SP3-2(FB)	500	500	1	250	3.5	19.5	3.5	–	–	0.44	2.94	1.747	2.729	0.330	300.5	300.5	300.5	0.447	III
SP3-4(FB)	500	500	1	250	3.5	37.0	3.5	–	–	0.53	1.49	0.775	2.729	0.330	300.5	300.5	300.5	0.522	IV
SP4-1(FB)	500	500	1	250	4.3	15.0	4.3	–	–	0.19	0.68	1.934	1.933	0.330	227.6	227.6	227.6	0.442	III
SP4-3(FB)	500	500	1	250	4.3	19.5	4.3	–	–	0.24	1.64	1.455	1.933	0.330	227.6	227.6	227.6	0.497	III
SP4-4(FB)	500	500	1	250	4.3	33.0	4.3	–	–	0.32	1.70	0.766	1.933	0.330	227.6	227.6	227.6	0.593	II
SP6-1(FB)	500	500	1	250	5.8	14.0	5.8	–	–	0.11	0.98	2.012	1.583	0.330	277.7	277.7	277.7	0.498	III
SP6-2(FB)	500	500	1	250	5.8	16.5	5.8	–	–	0.29	3.04	1.743	1.583	0.330	277.7	277.7	277.7	0.498	III
SP6-3(FB)	500	500	1	250	5.8	19.5	5.8	–	–	0.33	1.96	1.479	1.583	0.330	277.7	277.7	277.7	0.533	III
SP6-4(FB)	500	500	1	250	5.8	34.0	5.8	–	–	0.13	1.44	0.783	1.583	0.330	277.7	277.7	277.7	0.646	III

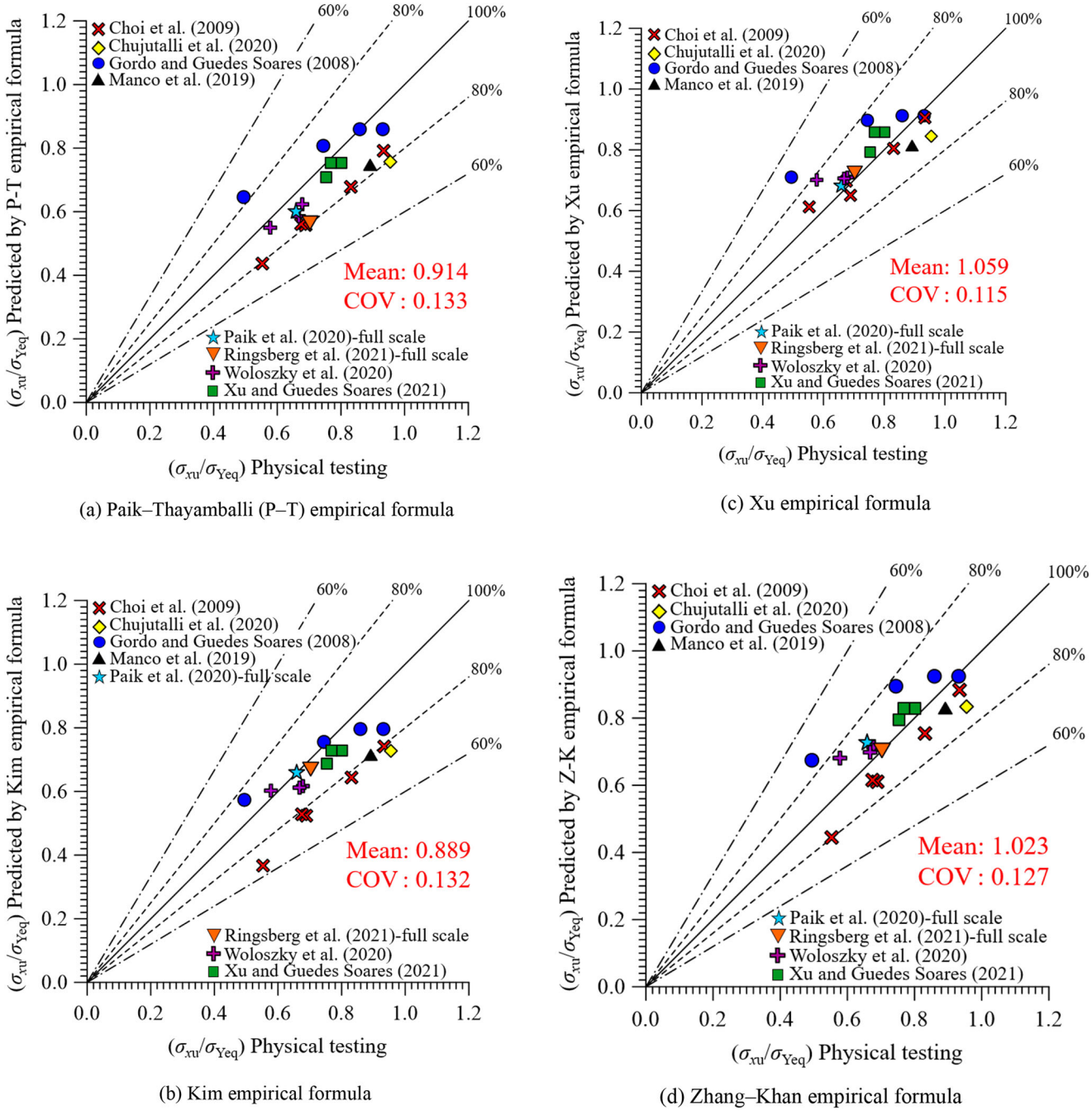

Figure 9. Comparison of the recent physical testing data and ultimate compressive strengths of stiffened panels predicted by various empirical formulae.

steel manufacturing and welding technologies. To this end, the Paik–Thayamballi empirical formula was applied to physical testing data reported since 1997. Moreover, analyses were conducted to compare the performance of the Paik–Thayamballi empirical formula applied to physical testing data with that of empirical formulae based on numerical simulations applied to the same data. The performances of all of the empirical formulae were quantitatively evaluated by calculating means and COVs of the data they generated. The results can be summarised as follows:

1) The maximum difference between the ultimate compressive strength of steel stiffened panels predicted by the Paik–Thayamballi empirical formula and the values obtained in recent testing studies was 10% in most cases.
2) The Paik–Thayamballi empirical formula yielded results that are in agreement with the full-scale physical testing data.
3) When applied to recent physical testing data, the Zhang–Khan empirical formula exhibited the lowest mean error (2.3%), followed by the Xu empirical formula (5.9%). Moreover, the values obtained using all the formulae are consistent with the recent physical testing data, as indicated by their acceptable COVs ($\leq$ 20%).
4) The recent and previous physical testing data have a similar profile, despite their diversity. The results generated by the Paik–Thayamballi empirical formula were not dependent on the year in which the testing data were acquired.
5) The Paik–Thayamballi empirical formula, which was developed in 1997 by fitting curves to testing data available up until that

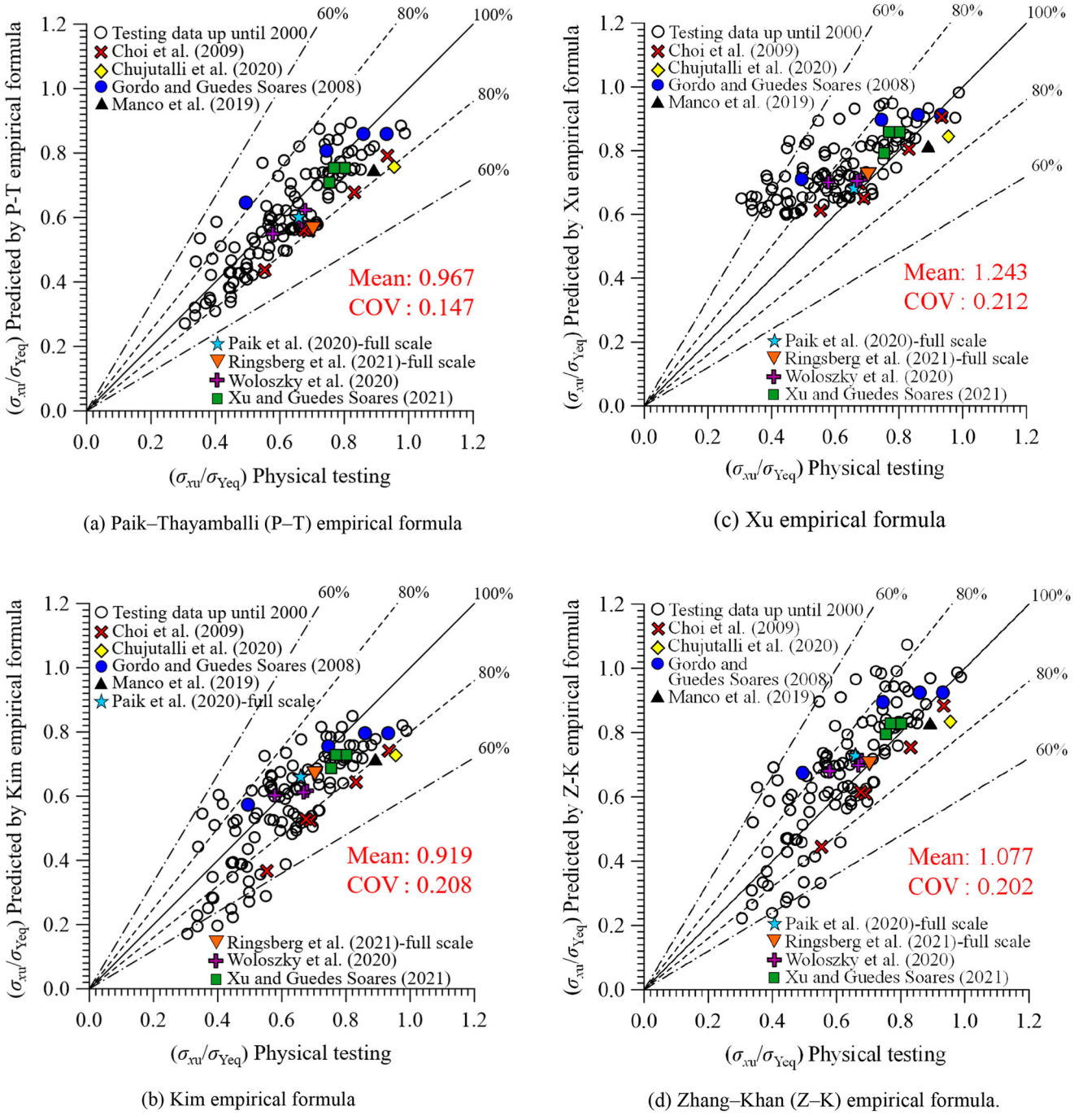

Figure 10. Comparison of physical testing data on ultimate compressive strengths of stiffened panels and that predicted by empirical formulae.

Table 8. Statistical analysis comparing ultimate compressive strengths obtained by various formulae using recent physical testing data, with and without previous physical testing data.

No.	Authors	Published	Database	Statistical measure	With only recent data	With recent and previous data
1	Paik and Thayamballi	1997	Physical testing	Mean	0.914	0.967
				COV	0.133	0.147
2	Kim et al.	2017	FEA	Mean	0.889	0.919
				COV	0.132	0.208
3	Xu et al.	2018	FEA	Mean	1.059	1.243
				COV	0.115	0.212
4	Zhang and Khan	2009	FEA	Mean	1.023	1.077
				COV	0.127	0.202

FEA = finite element analysis.

time, remains able to accurately predict the ultimate compressive strength of state-of-the-art steel stiffened panels. Despite the application of modern TMCP steels together with modern flux-cored arc welding technologies for fabrication.

The method with empirical formulae has a powerful advantage which can consider the effect of interaction between collapse modes in predicting the ultimate compressive strength of stiffened panels with a simple way. On the other hand, if some engineers want to predict the ultimate strength for each collapse mode, Common Structural Rules method or ALPS/ULSAP analytical method can be used (IACS 2022, ALPS/ULSAP 2021).

Acknowledgements

This study was supported by BK21 FOUR Graduate Program for Green-Smart Naval Architecture and Ocean Engineering of Pusan National University.

Disclosure statement

No potential conflict of interest was reported by the author(s).

ORCID

Jeom Kee Paik http://orcid.org/0000-0003-2956-9359

References

Abdussamie N, Ojeda R, Daboos M. 2018. Anfis method for ultimate strength prediction of unstiffened plates with pitting corrosion. Ships Offsh Struct. 13(5):540–550.

ALPS/ULSAP. 2021. A computer program for the ultimate limit state assessment of plates and stiffened panels. Greenboro, MD, USA: MAESTRO Marine LLC. www.maestromarine.com.

Anyfantis KN. 2020. Ultimate strength of stiffened panels subjected to non-uniform thrust. Int J Nav Archit Ocean Eng. 12:325–342.

Ao L, Wu H, Wang D, Wu W. 2020. Evaluation on the residual ultimate strength of stiffened plates with central dent under longitudinal thrust. Ocean Eng. 202:107167.

Bhudia K. 2019. Implementing the rotational restraint effects of surrounding support members into plate buckling strength design. Ships Offsh Struct. 14(5):457–468.

Choi BH, Hwang M, Yoon T, Yoo CH. 2009. Experimental study of inelastic buckling strength and stiffness requirements for longitudinally stiffened panels. Eng Struct. 31(5):1141–1153.

Chujutalli JH, Estefen SF, Soares CG. 2020. Indentation parameters influence on the ultimate strength of panels for different stiffeners. J Constr Steel Res. 170:106097.

Cui J, Wang D. 2020. An experimental and numerical investigation on ultimate strength of stiffened plates with opening and perforation corrosion. Ocean Eng. 205:107282.

Eslami-Majd A, Rahbar-Ranji A. 2015. Deformation behaviour of corroded plates subjected to blast loading. Ships Offsh Struct. 10(1):79–93.

Fanourgakis S, Samuelides M. 2021. Study of hull girder ultimate strength at elevated temperatures. Ships Offsh Struct. 16(sup1):186–203.

Faulkner D. 1977. *Compression tests on welded eccentrically stiffened plate panels*. Crosby Lockwood Staples. 130–139.

Feng GQ, Wang YT, Garbatove Y, Ren HL, Soares CG. 2021. Experimental and numerical analysis of crack growth in stiffened panels. Ships Offsh Struct. 16 (9):980–992.

Feng L, Hu L, Chen X, Shi H. 2020. A parametric study on effects of pitting corrosion on stiffened panels' ultimate strength. Int J Nav Archit Ocean Eng. 12:699–710.

Georgiadis DG, Samuelides MS. 2021. The effect of corrosion spatial randomness and model selection on the ultimate strength of stiffened panels. Ships Offsh Struct. 16(sup1):140–152.

Gordo JM, Guedes Soares C. 2008. Compressive tests on short continuous panels. Marine Structures. 21(2-3):113–137.

Han P, Ri K, Yun C, Pak C, Paek S. 2021. A study on the residual ultimate strength of continuous stiffened panels with a crack under the combined lateral pressure and in-panel compression. Ocean Eng. 234:109265.

He W, Cui X, Hu Z, Liu J, Wang C, Yao L. 2020. Probabilistic residual ultimate strength assessment of cracked unstiffened and stiffened plates under uniaxial compression. Ocean Eng. 216:108197.

Horne MR, Montague P, Narayanan R. 1977. Influence on strength of compression panels of stiffeners section. spacing and welded connection. Proc Inst Civ Eng. 63(1):1–20.

Horne MR, Narayanan R. 1976. Ultimate capacity of longitudinally stiffened plates used in box girders. Proceedings of the Institution of Civil Engineers. 61(2):253–280.

Hosseinabadi OF, Khedmati MR. 2021. A review on ultimate strength of aluminium structural elements and systems for marine applications. Ocean Eng. 232:109153.

Hughes OF, Paik JK. 2010. Ship structural analysis and design. The Society of Naval Architects and Marine Engineers. Alexandria, VA, USA.

IACS. 2022. Common structural rules for bulk carriers and oil tankers. London, UK: International Association of Classification Societies. www.iacs.org.uk.

Jagite G, Bigot F, Derbanne Q, Malenica Š, Sourne HL, Cartraud P. 2021. A parametric study on the dynamic ultimate strength of a stiffened panel subjected to wave- and whipping-induced stresses. Ships Offsh Struct. 16(9):1025–1039.

Jagite G, Bigot F, Derbanne Q, Malenica Š, Le Sourne H, Lauzon JD, Cartraud P. 2019. Numerical investigation on dynamic ultimate strength of stiffened panels considering real loading scenarios. Ships Offsh Struct. 14 (sup1):374–386.

Jagite G, Bigot F. 2022. Numerical investigation if the hull girder ultimate strength under realistic cyclic loading derived from long-term hydroelastic analysis. Ships Offsh Struct. doi:10.1080/17445302.2022.2035566.

Kim DK, Lim HL, Kim MS, Hwang OJ, Park KS. 2017. An empirical formulation for predicting the ultimate strength of stiffened panels subjected to longitudinal compression. Ocean Eng. 140:270–280.

Kim DK, Lim HL, Yu SY. 2018a. A technical review on ultimate strength prediction of stiffened panels in axial compression. Ocean Eng. 170:392–406.

Kim DK, Lim HL, Yu SY. 2019. Ultimate strength prediction of T-bar stiffened panel under longitudinal compression by data processing: A refined empirical formulation. Ocean Eng. 192:106522.

Kim DK, Poh BY, Lee JR, Paik JK. 2018b. Ultimate strength of initially deflected plate under longitudinal compression: part I-An advanced empirical formulation. Struct Eng Mech. 68(2):247–259.

Kim UN, Choe IH, Paik JK. 2009. Buckling and ultimate strength of perforated plate panels subject to axial compression: experimental and numerical investigations with design formulations. Ships Offsh Struct. 4(4):337–361.

Lee HH, Paik JK. 2020. Ultimate compressive strength computational modeling for stiffened plate panels with nonuniform thickness. J Mar Sci Appl. 19 (4):658–673.

Li D, Feng L, Huang D, Shi H, Wang S. 2021a. Residual ultimate strength of stiffened box girder with coupled damage of pitting corrosion and a crack under vertical bending moment. Ocean Eng. 235:109341.

Li S, Kim DK, Benson S. 2021b. The influence of residual stress on the ultimate strength of longitudinally compressed stiffened panels. Ocean Eng. 231:108839.

Lin YT. 1985. Ship longitudinal strength modeling. PhD. Thesis, Department of Naval Architecture and Ocean Engineering, University of Glasgow, Glasgow, Scotland.

Liu B, Gao L, Ao L, Wu W. 2021a. Experimental and numerical analysis of ultimate compressive strength of stiffened panel with openings. Ocean Eng. 220:108453.

Liu B, Yao X, Lin Y, Wu W, Guedes Soares C. 2021b. Experimental and numerical analysis of ultimate compressive strength of long-span stiffened panels. Ocean Eng. 237:109633.

Ma H, Wang D. 2021. Lateral pressure effect on the ultimate strength of the stiffened plate subjected to combined loads. Ocean Eng. 239:109926.

Manco MR, Vaz MA, Cyrino JCR, Ramos NM, Liang DA. 2019. Experimental and numerical study of uniaxially compressed stiffened plates with different plating thickness. Thin-Walled Struct. 145:106422.

Niho O. 1978. Ultimate strength of plated structures. Ph.D. Thesis, Department of Naval Architecture and Ocean Engineering, University of Tokyo, Japan.

Paik JK. 2018. Ultimate limit state analysis and design of plated structures. 2nd edition. Chichester, UK: John Wiley & Sons.

Paik JK. 2020. Advanced structural safety studies with extreme conditions and accidents. Singapore: Springer.

Paik JK. 2022. Ship-shaped offshore installations: design, construction, operation, healthcare and decommissioning. 2nd edition. Cambridge, UK: Cambridge University Press.

Paik JK, Lee DH, Noh SH, Park DK, Ringsberg JW. 2020a. Full-scale collapse testing of a steel stiffened plate structure under axial-compressive loading triggered by brittle fracture at cryogenic condition. Ships Offsh Struct. 15 (sup1):S29–S45.

Paik JK, Lee DH, Noh SH, Park DK, Ringsberg JW. 2020b. Full-scale collapse testing of a steel stiffened plate structure under cyclic axial-compressive loading. Structures. 26:996–1009.
Paik JK, Lee DH, Park DK, Ringsberg JW. 2021a. Full-scale collapse testing of a steel stiffened plate structure under axial-compressive loading at a temperature of −80°C. Ships Offsh Struct. 16(3):255–270.
Paik JK, Ryu MG, He K, Lee DH, Lee SY, Park DK, Thomas G. 2021b. Full-scale fire testing to collapse of steel stiffened plate structures under lateral patch loading (part 1) – without passive fire protection. Ships Offsh Struct. 16 (3):227–242.
Paik JK, Ryu MG, He K, Lee DH, Lee SY, Park DK, Thomas G. 2021c. Full-scale fire testing to collapse of steel stiffened plate structures under lateral patch loading (part 2) – with passive fire protection. Ships Offsh Struct. 16 (3):243–254.
Paik JK, Thayamballi AK. 1997. An empirical formulation for predicting the ultimate compressive strength of stiffened panels. Proceedings of the 7th International Offshore and polar Engineering conference, Honolulu, Hawaii, USA. 25-30 May.
Paik JK, Thayamballi AK. 2003. Ultimate limit state design of steel-plated structures. Chichester, UK: John Wiley & Sons.
Piculin S, Može P. 2021. Ultimate resistance of longitudinally stiffened curved plates subjected to pure compression. J Constr Steel Res. 181:106616.
Putranto T, Kõrgesaar M, Jelovica J, Tabri K, Naar H. 2021. Ultimate strength assessment of stiffened panel under uni-axial compression with non-linear equivalent single layer approach. Marine Struct. 78:103004.
Rahbar-Ranji A, Zarookian A. 2015. Ultimate strength of stiffened plates with a transverse crack under uniaxial compression. Ships Offsh Struct. 10(4):416–425.
Ringsberg JW, Darie L, Nahshon K, Shilling G, Vaz MA, Benson S, Brubak L, Feng G, Fujikubo M, Gaiotti M, et al. 2021. The ISSC 2022 committee III.1-ultimate strength benchmark study on the ultimate limit state analysis of a stiffened plate structure subjected to uniaxial compressive loads. Marine Struct. 79:103026.
Ryu MG, He K, Lee DH, Park SI, Thomas G, Paik JK. 2021. Finite element modeling for the progressive collapse analysis of steel stiffened-plate structures in fires. Thin-Walled Struct. 159:107262.
Shi GJ, Gao DW. 2021a. Ultimate strength of U-type stiffened panels for hatch covers used in ship cargo holds. Ships Offsh Struct. 16(3):280–291.
Shi GJ, Gao DW. 2021b. Transverse ultimate capacity of U-type stiffened panels for hatch covers used in ship cargo holds. Ships Offsh Struct. 16(6):608–619.
Shi XH, Hu Z, Zhang J, Guedes Soares C. 2021. Ultimate strength of a cracked stiffened panel repaired by CFRP and stop holes. Ocean Eng. 226:108850.
Sohn JM, Kim SJ, Seo JK, Kim BJ, Paik JK. 2016. Strength assessment of stiffened blast walls in offshore installations under explosions. Ships Offsh Struct. 11 (5):551–560.
Tanaka T, Endo H. 1988. Ultimate strength of stiffened plates with their stiffeners locally buckled in compression. Journal of the Society of Naval Architects of Japan. 1988 164:456–467.
Woloszyk K, Garbatov Y, Kowalski J, Samson L. 2020. Experimental and numerical investigations of ultimate strength of imperfect stiffened plates of different slenderness. Pol Marit Res. 27:120–129.
Xu MC, Soares CG. 2021. Experimental evaluation of the ultimate strength of stiffened panels under longitudinal compression. Ocean Eng. 220:108496.
Xu MC, Song ZJ, Pan J. 2021. Study on the similarity methods for the assessment of ultimate strength of stiffened panels under axial load based on tests and numerical simulations. Ocean Eng. 219:108294.
Xu MC, Song ZJ, Zhang BW, Pan J. 2018. Empirical formula for predicting ultimate strength of stiffened panel of ship structure under combined longitudinal compression and lateral loads. Ocean Eng. 162:161–175.
Xu W, Zhou X, Li C, Ren H. 2019. Post-ultimate strength behaviour and collapse severity of ship hull girder under extreme wave load by an analytical method. Ships Offsh Struct. doi: 10.1080/17445302.2020.1834753.
Yao T. 1980. Ultimate compressive strength of ship platings. Ph.D. Thesis, Department of Naval Architecture and Ocean Engineering, University of Tokyo, Japan.
Yi MS, Hyun CM, Paik JK. 2019. An empirical formulation for predicting welding-induced biaxial compressive residual stresses on steel stiffened plate structures and its application to thermal plate buckling prevention. Ships Offsh Struct. 14(sup1):18–33.
Yi MS, Lee DH, Lee HH, Paik JK. 2020. Direct measurements and numerical predictions of welding-induced initial deformations in a full-scale steel stiffened plate structure. Thin-Walled Structures. 153:106786.
Yi MS, Noh SH, Lee DH, Seo DH, Paik JK. 2021. Direct measurements, numerical predictions and simple formula estimations of welding-induced biaxial residual stresses in a full-scale stiffened plate structure. Structures. 29:2094–2105.
Zhang J, Shi XH, Soares C, Liu J. 2020. Ultimate strength of stiffened panels with a crack and pits under uni-axial longitudinal compression. Ships Offsh Struct. doi: 10.1080/17445302.2020.1827805.
Zhang S. 2014. A review and study on ultimate strength of steel plates and stiffened panels in axial compression. Ships Offsh Struct. 11(1):81–91.
Zhang S, Khan I. 2009. Buckling and ultimate capability of plates and stiffened panels in axial compression. Marine Structures. 22(4):791–808.